Evaluation of Hybrid Positioning Scenarios for Autonomous Vehicle Applications

José A. del Peral-Rosado(1), Roger Estatuet-Castillo(1), José A. López-Salcedo(1) , Gonzalo Seco-Granados(1),
Zdenek Chaloupka(2), Lionel Ries(2), and José A. García-Molina(2,3)
(1) *Dept. of Telecommunications and Systems Engineering, Universitat Autònoma de Barcelona (UAB), Bellaterra, Spain*
(2) *European Space Agency (ESA), Noordwijk, The Netherlands*
(3) *HE Space, Noordwijk, The Netherlands*
e-mails: JoseAntonio.DelPeral@uab.cat, Roger.Estatuet@uab.cat, Jose.Salcedo@uab.cat, Gonzalo.Seco@uab.cat,
Zdenek.Chaloupka@esa.int, Lionel.Ries@esa.int, Jose.Antonio.Garcia.Molina@esa.int

BIOGRAPHY

Dr. **José A. del Peral-Rosado** received the Ph.D. degree on Telecommunications Engineering from Universitat Autònoma de Barcelona (UAB) in 2014. Since 2014, he is a Postdoctoral Researcher at the Department of Telecommunications and Systems Engineering at UAB. From 2014 to 2016, he was a Visiting Researcher at the European Space Research and Technology Centre (ESTEC) of the European Space Agency (ESA). His research interests are in satellite and terrestrial localization and navigation.
Roger Estatuet Castillo received the B.Sc. in Telecommunication Engineering in 2016 from Universitat Autònoma de Barcelona (UAB) and he is currently completing the M.Sc. in Telecommunication Systems from Universitat Oberta de Catalunya (UOC). He is a radionavigation engineer at ESA/ESTEC, contracted by Universitat Autònoma de Barcelona (UAB).
Prof. **José A. López-Salcedo** received the M.Sc. and Ph.D. degrees in Telecommunication Engineering in 2001 and 2007, respectively, from Universitat Politècnica de Catalunya (UPC). From 2002 to 2006, he was a Research Assistant at UPC involved in R+D projects related with synchronization techniques for digital receivers, satellite communications and iterative decoding techniques for MIMO wireless systems, both for private industry and public administrations. Since 2006, he is Assistant Professor at the Department of Telecomunications and Systems Engineering, Universitat Autònoma de Barcelona (UAB), and member of the SPCOMNAV group.
Prof. **Gonzalo Seco-Granados** received the Ph.D. degree in Telecommunications Engineering from the Universitat Politècnica de Catalunya, in 2000, and the MBA degree from IESE Business School, in 2002. Until 2005, he was with the European Space Agency, involved in the design of the Galileo System. Since 2006, he has been an Associate Professor with the Department of Telecommunications, Universitat Autònoma de Barcelona. In 2015, he was a Fulbright Visiting Scholar with the University of California, Irvine. He has been general co-chair of ICL-GNSS'2016 and executive co-chair of ASMS/SPSC'2016. His research interests include the design of signals and reception techniques for satellite and terrestrial localization systems, multi-antenna receivers, and positioning with 5G technologies.
Dr. **Zdenek Chaloupka** received his M.S. and Ph.D. degrees from the Czech Technical University in Prague in 2005 and 2009, respectively, both in electrical engineering. He is currently with the European Space Agency (ESA), European Space Research and Technology Centre (ESTEC), where he works on research topics related to time synchronization and high accuracy positioning using satellite navigation systems and next generation mobile networks (5G).
Lionel Ries is a Radio Navigation engineer at ESA/ESTEC in Noordwijk, The Netherlands. He has lead R&D activities on signal design and processing, receivers and payloads regarding location, and navigation systems including GNSS (Galileo, GNSS space receivers), search & rescue by satellite (SARSAT, MEOSAR), and Argos (Advanced Data Collect and Location by Satellite, mostly for environment and widelife monitoring). He was head of the location/navigation signal department in CNES, the French Space Agency.
José A. García-Molina is a Radio Navigation engineer at ESA/ESTEC in Noordwijk, The Netherlands, where he leads several R&D projects and internal research activities on GNSS receiver technology and signal processing techniques for ground and space applications in the context of different ESA programs (including Galileo). His main research interests include signal processing and estimation theory, GNSS/Galileo receivers and signals, hybrid and cooperative/collaborative positioning, array signal processing, identification and localization of jammers/spoofers, SDR receivers, and cloud positioning techniques and applications.

ABSTRACT

Autonomous vehicle applications, such as assisted driving, collision avoidance or platooning, demand precise, reliable and secure localization in harsh environments such as tunnels and urban areas. In order to solve these positioning challenges, multiple navigation technologies have to be fused. These technologies are typically based on Global Navigation Satellite Systems (GNSS), radar, camera, inertial sensors and signals of opportunity. Indeed, the exploitation of cellular communications for positioning is of special interest due to the advanced physical features of fourth generation (4G) and fifth generation (5G) mobile networks. The objective of this work is to assess the nominal performance of hybrid GNSS and 4G Long Term Evolution (LTE) solutions, based on assisted or opportunistic approaches. For this purpose, a software tool is presented to evaluate different hybrid scenarios, by using field GNSS and simulated LTE observables. The assisted LTE approach is shown to outperform the opportunistic approach, by avoiding network inaccuracies. The proposed hybrid solutions achieve full position availability with a position accuracy around 10 meters at the 95% of the cases in urban and road scenarios. Future work is still necessary to fulfil the stringent location requirements of autonomous vehicle applications, by adopting a hybrid fusion of advanced technologies such as 5G networks, precise GNSS and inertial sensors.

1 INTRODUCTION

Navigation systems have a key role in autonomous vehicles to fulfil road safety and efficient mobility requirements. Emerging vehicular applications, such as assisted driving, collision avoidance or platooning, demand high accuracy and reliable vehicle location [1]. Thus, the fusion of Global Navigation Satellite Systems (GNSS) with relative positioning technologies, such as radars, signals of opportunity, cameras and inertial sensors, is typically considered the main candidate solution for autonomous navigation. These hybrid or multi-sensor technologies aim at complementing and enhancing GNSS, especially for those critical situations with a lack of satellite visibility, such as in tunnels and urban canyons. The use of signals of opportunity from terrestrial communication systems is of special interest to provide additional ranging measurements for trilateration. However, the lack of information from these terrestrial transmitters, such as the transmitter position or the transmission time, may prevent high-accuracy and reliable positioning. Thus, dedicated terrestrial positioning signals are preferred to be used in the navigation fusion. This is the case of dedicated pilots standardized in current fourth generation (4G) Long Term Evolution (LTE) cellular networks [2], i.e., positioning reference signal (PRS). The use of these signals in vehicle-to-everything (V2X) cellular networks is specially attractive to provide vehicular localization. Furthermore, disruptive technologies considered in future fifth generation (5G) networks are envisaged to considerably enhance the achievable cellular-based vehicular localization [3]. However, the standardization bodies have not yet defined network-based positioning methods dedicated to assist the navigation fusion in autonomous vehicles.

Until now, cellular location requirements were mainly demanded for emergency and location-based services, which have motivated the standardization of cellular location methods. In 2015, a horizontal position accuracy of 50 meters was mandated for E911 emergency calls [4]. As a result, the 3rd Generation Partnership Project (3GPP) studied in [5] the indoor positioning capabilities of the LTE standard to fulfil this mandate. However, the additional infrastructure required to ensure tight network synchronization has prevented the adoption of observed time-difference of arrival (OTDoA) with PRS in commercial LTE deployments, making GNSS and enhanced-cell ID (E-CID) the main location methods exploited [6]. Thus, opportunistic approaches have been presented as an alternative to exploit the LTE transmissions for positioning. In [7], opportunistic positioning based on an initial known receiver position is validated with laboratory experiments. Field measurements are conducted in two different vehicular scenarios in [8] and [9, 10]. Their results show a position accuracy around 10 meters for LTE system bandwidths between 10 and 20 MHz. The main drawbacks of these opportunistic techniques are the need to estimate the network synchronization, the precision of the base stations (BS) locations, and the hearibility problem of neighbour BSs.

The hybrid fusion of GNSS and cellular systems have also been studied in the literature. An analytical analysis is provided in [11] by considering a hybrid approach with very few GNSS and cellular signals available. In [12], GNSS and 3G cellular systems are integrated in a loosely-coupled architecture, where the location is computed either with the satellite or terrestrial system depending on the signal availability, and the Manhattan grid is used in the simulation results. The hybrid GNSS and LTE performance is simulated for urban environments in [13], by considering ray-tracing models and a 20-MHz LTE signal bandwidth. A methodology to evaluate hybrid GNSS and LTE methods in representative urban scenarios is proposed in [14], by combining field GNSS and simulated LTE measurements. The results of these contributions show the importance of using additional ranging measurements when there is a lack of visible satellites. Preliminary results on vehicle-to-vehicle (V2V) aided GNSS localization are shown in [15]. However, to the best of authors' knowledge, there is no study on the achievable performance of assisted and opportunistic hybrid localization for autonomous vehicle applications, by using multi-GNSS and LTE vehicle-to-infrastructure (V2I) communications, where the assistance data (i.e., location of LTE BSs and network synchronization) is provided by the network through a non-standard protocol.

The objective of this work is to propose and evaluate general hybrid GNSS and cellular V2I positioning scenarios, in order to assess the critical aspects on the fulfilment of accurate and reliable navigation for autonomous vehicles, especially in urban environments. As a result of the tightly-coupled hybrid fusion of GNSS and cellular V2I pseudoranges, potential requirements for 4G and 5G cellular networks are recommended. For this purpose, a novel software tool is implemented to post-process field GNSS and simulated LTE pseudoranges for assisted and opportunistic hybrid positioning, in contrast to existing tools based only in GNSS, such as the goGPS project [16]. In the assisted approach, the vehicle is assumed to be subscribed to a network operator that securely provides location-related information, such as the position of the BSs and its transmission time, while in the opportunistic approach, the receiver coarsely knows or needs to estimate those network parameters. In both approaches, the navigation engine is assumed to be implemented at the vehicle receiver, in order to allow the integration of additional technologies for positioning, such as cameras, radars or inertial sensors. The hybrid positioning performance is then evaluated for urban street and road scenarios.

The outline of the paper is as follows: Section 2 introduces a software tool to evaluate the hybrid positioning performance, Section 3 describes general hybrid scenarios identified for vehicular localization, Section 4 shows the performance results and recommends potential requirements, and Section 5 draws the conclusions and future work.

2 HYBRID POSITIONING EVALUATION TOOL

This section describes a novel positioning software tool, called *HybUAB*, which is able to evaluate the hybrid GNSS and LTE V2I positioning performance in vehicular scenarios. This tool post-processes field GNSS pseudoranges and simulates LTE measurements, in order to compute their stand-alone or hybrid positioning solution over a reference receiver trajectory. The objective of this tool is to assess the achievable hybrid positioning performance, by using assisted or opportunistic approaches with LTE signals. The integration of a physical-layer LTE positioning software receiver, which is described in [7] and [17], is left for future work.

The HybUAB platform is defined by three main blocks, as it is shown in Figure 1. The pre-processing module analyses the GNSS raw data and simulates the LTE ranging estimates, by using the reference trajectory of the receiver, a database of BS locations and predefined propagation models. Then, the hybrid navigation engine uses these ranging measurements to compute the position, velocity and time (PVT) solution, by considering the configuration parameters of the platform. Finally, the position accuracy and availability is evaluated, given a certain scenario definition.

2.1 Pre-processing Module

The pre-processing module is aimed at preparing the GNSS and LTE pseudoranges for the calculation of the receiver location, and at configuring the platform to evaluate the accuracy and reliability of the position fix. The main inputs of this module are the reference trajectory of the receiver, the GNSS observables and navigation data, the database of LTE BSs, and the LTE simulation parameters.

The reference trajectory is used to evaluate the positioning performance and to generate the LTE time-of-arrival (ToA) pseudoranges. Thus, this reference data needs to have a good precision, in order to ensure the validity of the evaluation results.

The GNSS raw data can be obtained from mass-market receivers, professional receivers, GNSS reference stations (GRS) or commercial mobile devices, such as Android phones. The observable and navigation files typically use the receiver independent exchange (RINEX) format, but additional formats can be supported with specific parsers. The navigation data can also be

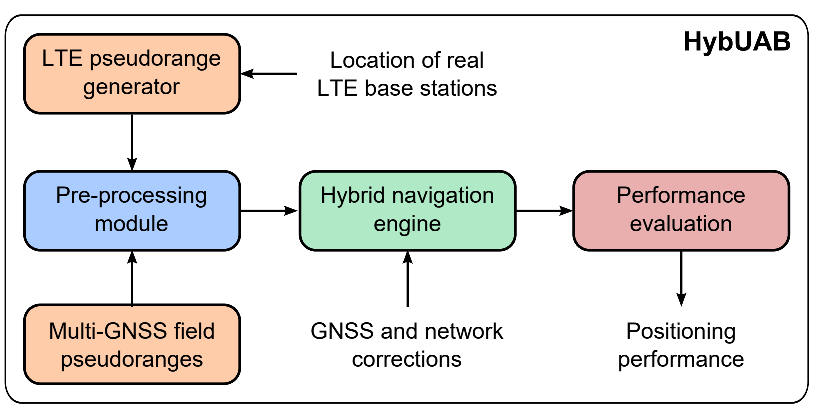

Fig. 1 Overall description of the HybUAB platform.

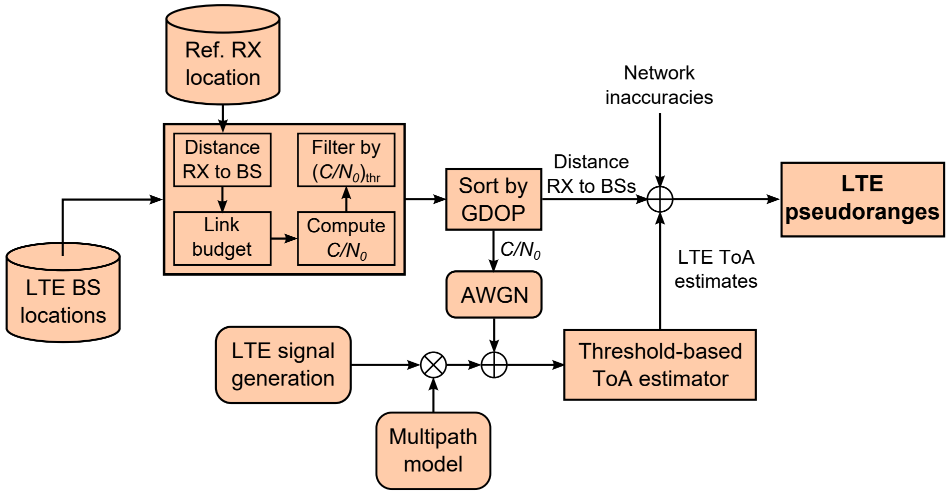

Fig. 2 Overall architecture of the 4G LTE pseudorange generator [14].

obtained from public GNSS services, such as the international GNSS service (IGS). The GNSS observables are obtained from multiple constellations, and they are processed for the epochs under study, in order to determine the satellite visibility conditions. These pseudoranges are then corrected according to the navigation data available. The ionospheric corrections are based on the Klobuchar model [18, pp. 301–303], the tropospheric corrections use the Saastamoinen algorithm [19], and satellite clock and orbit corrections are computed with broadcast ephemeris, such as in [20]. The use of precise navigation corrections is left for future work.

The multi-GNSS pseudoranges are expected to be obtained from a field campaign of measurements, where the receiver has a dynamic trajectory. But, the HybUAB platform also includes a functionality to mask pseudoranges according to a certain predefined elevation. As it is described in [14], urban elevation masks, which can be obtained from three-dimensional (3D) city models or a fish-eye camera, can also be applied to open-sky field measurements from GRS static locations, in order to emulate urban environments. In addition, simulated GNSS pseudoranges, such as in [21], can also be used as input for the software tool.

The generation of LTE ToA pseudoranges is based on the simulation process described in [14], as it is shown in Figure 2. The reference trajectory is used to calculate the distance between the closest BSs and the receiver. The 3D coordinates of these BSs are obtained from a public database of commercial BSs from different network operators. The distances between receiver and BSs are used to calculate the link budget with standard propagation models [22]. The link budget from each BS determines the signal-to-noise ratio (SNR), which is used to select the most powerful BSs with the best horizontal dilution of precision (HDOP). Considering the detected BSs, the corresponding noise contribution is added after the convolution between LTE transmitted signals and the multipath channel. This procedure is repeated for each BS to simulate the received LTE signals. Then, a conventional threshold-based time-delay estimator is used at the receiver to obtain the simulated ranging measurements. Additional ranging errors due to network impairments, such as BS location and network synchronization errors, can then be introduced.

2.2 Hybrid Navigation Engine

The hybrid navigation engine computes the vehicle location based on a snapshot algorithm or a navigation algorithm. The snapshot algorithm calculates the position based only on the current epoch of GNSS and LTE measurements. This algorithm is implemented based on the solution of the least-squares (LS) or weighted LS (WLS) problem, by means of a Gauss-Newton (GN) solver. The navigation algorithm computes, filters and predicts the position solution, by means of an extended Kalman filter (EKF). These positioning algorithms are briefly described in this section.

Snapshot Algorithm: LS and WLS

Let us consider N location systems with a total number of GNSS and LTE transmitters equal to

$$L = \sum_{n=1}^{N} M_n, \tag{1}$$

where M_n is the number of transmitters for the n-th system. Since each system operates in a certain frequency band, the RF front-end may introduce a different clock offset for each system. Thus, additional unknowns have to be added for the hybrid location problem, resulting in $\boldsymbol{\theta}_{\text{hyb}} = [x, y, z, \boldsymbol{\delta}\mathbf{t}]^{\text{T}}$ with $\boldsymbol{\delta}\mathbf{t} = [\delta t_1, \ldots, \delta t_Q]$ for $Q \leq N$ clock offsets. Thus, the hybrid GN solution at the ℓ-th iteration is

$$\hat{\boldsymbol{\theta}}_{\text{hyb}}(\ell) = \hat{\boldsymbol{\theta}}_{\text{hyb}}(\ell - 1) + \left(\mathbf{H}^{\text{T}}\mathbf{W}\mathbf{H}\right)^{-1}\mathbf{H}^{\text{T}} \cdot \mathbf{W} \cdot \hat{\mathbf{e}}_{\text{hyb}}, \tag{2}$$

where $\hat{\mathbf{e}}_{\text{hyb}} = \boldsymbol{\rho}_{\text{hyb}} - \hat{\boldsymbol{\rho}}_{\text{hyb}}$, being $\boldsymbol{\rho}_{\text{hyb}} = [\rho_1, \ldots, \rho_L]^{\text{T}}$ and $\hat{\boldsymbol{\rho}}_{\text{hyb}} = [\hat{\rho}_1, \ldots, \hat{\rho}_L]^{\text{T}}$ the observed and approximate pseudoranges of multiple systems, respectively. The hybrid geometry matrix is defined by

$$\mathbf{H} = \begin{bmatrix}\mathbf{A}_{xyz} & -\mathbf{A}_{\delta t}\end{bmatrix}, \tag{3}$$

where the Jacobian matrix of the 3D location is

$$\mathbf{A}_{xyz} = [\mathbf{a}_1, \ldots, \mathbf{a}_m, \ldots, \mathbf{a}_L]^{\text{T}}, \tag{4}$$

being $\mathbf{a}_m = \begin{bmatrix}\frac{x_m - \hat{x}}{\hat{\rho}_m} & \frac{y_m - \hat{y}}{\hat{\rho}_m} & \frac{z_m - \hat{z}}{\hat{\rho}_m}\end{bmatrix}^{\text{T}}$, and the Jacobian matrix of the clock offsets $\mathbf{A}_{\delta t}$ is a $L \times Q$ matrix filled with ones for any m-th pseudorange corresponding to the q-th clock and filled with zeros otherwise, e.g.,

$$\mathbf{A}_{\delta t} = \begin{bmatrix}\mathbf{1}_{M_1\times 1} & \mathbf{0}_{M_1\times 1} & \cdots & \mathbf{0}_{M_1\times 1}\\ \mathbf{0}_{M_2\times 1} & \mathbf{1}_{M_2\times 1} & \cdots & \mathbf{0}_{M_2\times 1}\\ \vdots & \vdots & \ddots & \vdots\\ \mathbf{0}_{M_Q\times 1} & \mathbf{0}_{M_Q\times 1} & \cdots & \mathbf{1}_{M_Q\times 1}\end{bmatrix} \tag{5}$$

for $Q = N$, being $\mathbf{1}$ and $\mathbf{0}$ vector of ones and zeros, respectively. Thus, the number of observed pseudoranges required to compute the hybrid solution is $L \geq 3 + Q$. For the LS algorithm, the weighting matrix $\mathbf{W}$ is equal to the identity matrix $\mathbf{I}_{L\times L}$, and for the WLS algorithm, it is written as

$$\mathbf{W} = \begin{bmatrix}w_1 & & \mathbf{0}\\ & \ddots & \\ \mathbf{0} & & w_L\end{bmatrix}, \tag{6}$$

where these weights are defined by the measurement quality of the L ranging measurements, e.g. based on the carrier-to-noise-density ratio (C/N_0), satellite elevation or non-line-of-sight (NLoS) conditions.

Navigation Algorithm: EKF

The EKF algorithm is based on three main steps:

- **Initialisation**: The state vector is first initialized as

$$\hat{\mathbf{x}}_{\mathbf{0}} = \begin{bmatrix}x & v_x & y & v_y & z & v_z & \boldsymbol{\delta}_t & \dot{\boldsymbol{\delta}}_t\end{bmatrix}^{\text{T}}, \tag{7}$$

  where x, y, z are the approximate ECEF coordinates of the vehicle position, v_x, v_y, v_z are the corresponding approximate velocities, $\boldsymbol{\delta}_t$ is the approximate clock offset vector between the GNSS or LTE systems and the receiver, and $\dot{\boldsymbol{\delta}}_t$ is the corresponding approximate clock drift vector. The state vector covariance matrix is also initialised as

$$\mathbf{P}_{\mathbf{0}} = \begin{bmatrix}\sigma_1^2 & & \mathbf{0}\\ & \ddots & \\ \mathbf{0} & & \sigma_P^2\end{bmatrix}, \tag{8}$$

  where σ_p^2 is the initial variance for the p-th state, and the total number of states is $P = 2 \cdot (Q + 3)$.

- **Prediction**: After the initialisation, the state vector is computed at the k-th epoch as

$$\hat{\mathbf{x}}_k^- = \mathbf{F} \cdot \hat{\mathbf{x}}_{k-1}, \tag{9}$$

  where transition matrix is a block diagonal matrix defined as

$$\mathbf{F} = \mathbf{I}_{P/2\times P/2} \otimes \begin{bmatrix}1 & T_c\\ 0 & 1\end{bmatrix}, \tag{10}$$

being the Kronecker product denoted by $\otimes$, and T_c the time interval between epochs. The state vector covariance matrix is then predicted as

$$\mathbf{P}_k^- = \mathbf{F} \cdot \mathbf{P}_{k-1} \cdot \mathbf{F}^\mathbf{T} + \mathbf{Q}, \tag{11}$$

where $\mathbf{Q}$ is the state transition noise covariance matrix or state covariance matrix, which is defined as

$$\mathbf{Q} = \begin{bmatrix} \mathbf{I}_{3\times3} \otimes \mathbf{Q}_\mathbf{pv} & \mathbf{0} \\ \mathbf{0} & \mathbf{I}_{Q\times Q} \otimes \mathbf{Q}_\mathbf{t} \end{bmatrix}. \tag{12}$$

The covariance matrix of the position and velocity is

$$\mathbf{Q}_\mathbf{pv} = \sigma_\mathrm{pv}^2 \cdot \begin{bmatrix} T_c^3/2 & T_c^2/2 \\ T_c^2/2 & T_c \end{bmatrix}, \tag{13}$$

and the covariance matrix of the clock offsets and clock drifts is

$$\mathbf{Q}_\mathbf{t} = \begin{bmatrix} \sigma_\mathrm{t}^2 T_c + \sigma_\mathrm{dt}^2 T_c^3/3 & \sigma_\mathrm{dt}^2 T_c^2/2 \\ \sigma_\mathrm{dt}^2 T_c^2/2 & \sigma_\mathrm{dt}^2 T_c \end{bmatrix}, \tag{14}$$

where σ_pv is the standard deviation of the position, σ_t is the standard deviation of the clock offset, and σ_dt is the standard deviation of the clock drift.

- **Update**: The predicted state vector is then updated with the weighted prediction error as,

$$\hat{\mathbf{x}}_k = \hat{\mathbf{x}}_k^- + \mathbf{K}_k \cdot (\mathbf{z}_k - \mathbf{H} \cdot \hat{\mathbf{x}}_k^-), \tag{15}$$

where $\mathbf{z}_k$ is the observable vector, $\mathbf{H}$ is the Jacobian matrix of the state vector, and $\mathbf{K}_k$ is the Kalman gain matrix, defined as

$$\mathbf{K}_k = \mathbf{P}_k^- \cdot \mathbf{H}^T \cdot (\mathbf{H} \cdot \mathbf{P}_k^- \mathbf{H}^T + \mathbf{R})^{-1}, \tag{16}$$

being $\mathbf{R}$ the measurement covariance matrix. Using (4) and (5), the Jacobian matrix $\mathbf{H}$ of the EKF is expressed as

$$\mathbf{H} = \begin{bmatrix} \mathbf{A}_{xyz} \otimes \begin{bmatrix} 1 & 0 \end{bmatrix} & -\mathbf{A}_{\delta t} \otimes \begin{bmatrix} 1 & 0 \end{bmatrix} \end{bmatrix}. \tag{17}$$

Finally, the state covariance matrix is updated as

$$\mathbf{P}_k = (\mathbf{I}_{P\times P} - \mathbf{K}_k \cdot \mathbf{H}) \cdot \mathbf{P}_k^-. \tag{18}$$

2.3 Performance Metrics

The performance evaluation of the hybrid positioning platform is based on the root-mean-square-error (RMSE) of the estimated position, the cumulative density function (CDF) of the position error, the geometry of the position problem with the HDOP, and the probability of position fix. The position error is only assessed in the horizontal dimension of the vehicle, i.e., two-dimensional (2D) error, in order to assess the positioning performance for autonomous vehicle applications, which mainly require lane detection and high-accuracy distance between vehicles.

3 HYBRID EVALUATION SCENARIOS

This section describes three different scenarios to evaluate the positioning performance of hybrid GNSS and LTE algorithms based on assisted and opportunistic approaches, by using the HybUAB platform. The definition of these scenarios is mainly based on the satellite visibility, i.e., full, partial, low and no visibility, as it is can be seen in Table 1, and on the positioning approach, i.e., assisted or opportunistic.

3.1 Scenario 1: Cell Site Mapping

The objective of this scenario is to assess the positioning capabilities of an opportunistic LTE receiver to locate unknown cellular transmitters. This lack of knowledge may be, for instance, due to a BS operated by a non-collaborative network provider, or a mobile transmitter, such as another vehicle. Since the vehicle may move around the transmitter, the location of the transmitter can be estimated over time, by considering the precise vehicle position obtained with a multi-GNSS receiver over full visibility conditions.

Table 1 Definition of the GNSS visibility status according to the number of visible satellites.

Constellation	Full visibility	Partial visibility	Low visibility	No visibility
GNSS	≥ 11	≥ 6 (up to 10)	≤ 5	0
GPS	≥ 8	≥ 3 (up to 7)	≤ 2	0
Galileo	≥ 3	2	1	0
GLONASS	≥ 3	2	1	0

3.2 Scenario 2: Two-step Multi-GNSS Positioning

The objective of this scenario is to assess the performance of two-step multi-GNSS positioning. The GNSS assistance data, such as the clock offset between GNSS constellations, may be provided by an external source or may be estimated during epochs with good satellite visibility. One of the main improvements is by reducing the number of state parameters to be estimated by the positioning algorithm. For instance, the 3D position solution with three GNSS constellations may require a minimum of six pseudoranges, while the assisted solution may only require three pseudoranges, by re-using the estimated GPS to Galileo time offset (GGTO), GPS-to-GLONASS time offset, vehicle height and velocity. This work focuses on the evaluation of a two-step approach, based on the estimation and re-use of the clock offset between multiple constellations, by means of a snapshot WLS positioning algorithm.

3.3 Scenario 3: Hybrid Navigation

The objective of this scenario is to assess the positioning performance of the hybrid multi-GNSS and LTE solution with the assisted and opportunistic approaches. The opportunistic hybrid positioning solution is evaluated by introducing a representative error on the location and network synchronization of the cellular BS, while the assisted approach does not include these network inaccuracies. In both cases, the reference time of the LTE network is not required to be equal to the GPS time. The fusion of multi-GNSS and cellular V2I pseudoranges is necessary to provide an accurate and reliable vehicle position. The performance evaluation of this scenario is based on an EKF navigation algorithm. The EKF implementation with a reduction of estimation parameters, as studied in the two-step approach of scenario 2, is left for future work.

4 PERFORMANCE EVALUATION

This section summarizes the performance results for the different hybrid evaluation scenarios. In addition, future requirements on GNSS, 4G and 5G systems are recommended for autonomous vehicle applications, based on the results obtained by the HybUAB platform.

4.1 Testbed Definition

The evaluation of the hybrid vehicle localization is performed by post-processing field GNSS data collections and simulated LTE V2I measurements. The field campaign of GNSS pseudoranges is conducted over urban street and road scenarios, as it is shown in Figure 3 by mapping the vehicle trajectory. The main parameters of the field GNSS data collections, as well as the expected number of detected LTE BSs, are summarized in Table 2.

The GNSS raw observables of the two field campaigns are obtained by a single-frequency professional GNSS receiver, integrated in the navigation van of the European Space Agency (ESA). The field campaigns are conducted over urban street and road scenarios in The Hague (The Netherlands). In both cases, the GNSS constellations supported are GPS, Galileo, and GLONASS. The reference vehicle position is obtained with the professional NovAtel SPAN receiver, which is based on a GNSS+INS solution able to achieve a position accuracy below a meter. Broadcast ephemeris are used to compute the PVT solution.

The simulation of the LTE raw data is based on the procedure defined in [14], and described in Section 2.1. One of the main inputs is the location of the 4G LTE BSs. The public database of the Dutch antenna bureau [23] is here used to obtain the real location of commercial LTE BSs deployed by different network providers in The Netherlands. These BS positions are provided in World Geodetic System 1984 (WGS84) coordinates with a location accuracy of 15 meters. The main simulation parameters are based on a macro-cell deployment, where the average transmit power is equal to 43 dBm and the carrier frequency is set to 816 MHz with a bandwidth of 10 MHz. The multipath channel is simulated with the extended typical urban (ETU) model [24], which is the standard multipath model used to represent urban scenarios with a high delay spread (i.e., equal to 5μs). A distance-dependent line-of-sight (LoS) model is also considered by ensuring a certain LoS probability as function of the

Table 2 Description of the field GNSS data collections.

Scenarios	Road	Urban street
Location	The Hague, The Netherlands	
Date	10/03/2016	25/04/2016
Type of receiver	Single-frequency professional	
GNSS antenna	NovAtel GPS-704-WB	
Reference trajectory	NovAtel SPAN receiver	
Epoch interval	1 second	
Number of epochs	1196	9590
Full GNSS	48.72%	35.79%
Partial GNSS	48.30%	53.10%
Low GNSS	2.65%	10.99%
No GNSS	0.32%	0.12%
Detected LTE BSs	117	134

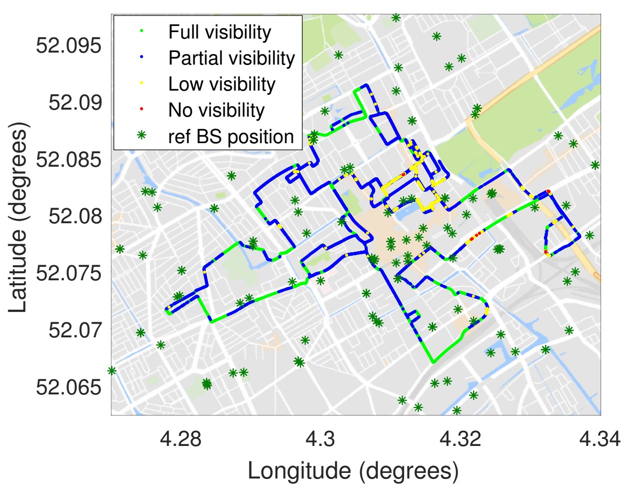

(a) Urban street trajectory.

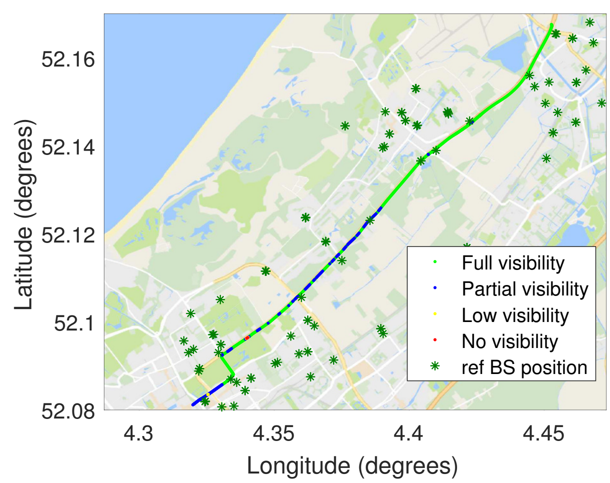

(b) Road trajectory.

Fig. 3 Map of the vehicle trajectory during the field GNSS campaigns.

distance between BS and vehicle [14]. A conventional time-delay estimator, i.e., first-peak or threshold-based estimator, is used with a heuristic threshold equal to 6 dB, as in [14]. For each GNSS epoch, LTE ToA measurements are generated from four or eight BSs, depending if a low-density or high-density network is simulated, respectively. In both assisted and opportunistic approaches, the inter-cell interference is assumed to be avoided with the PRS or with transmissions at different frequency bands. The HybUAB platform is able to post-process the GNSS and LTE data for the different scenarios defined in Section 3. For this purpose, the location algorithms are configured accordingly for each scenario:

- **Cell site mapping configuration**: The position estimation of each detectable BS is implemented based on a LS algorithm, by considering the entire set of LTE downlink measurements received from the detected BS, i.e., from past epochs to the present one as the vehicle moves around the BS of interest. Thus, the vehicle location is assumed to be known, and equal to the reference position. The LS algorithm is able to converge to the BS location with an initial coarse BS position, provided by the maximum cell coverage. This preliminary implementation already provides a representative BS location accuracy of opportunistic approaches. Future work is aimed at using the EKF solution for the cell site mapping.

- **Multi-GNSS configuration**: The WLS algorithm is configured to estimate the 3D position and the receiver clock offset with respect to each GNSS constellation, resulting in a maximum of six estimation parameters. These clock offsets are first estimated, and then re-used to reduce the number of estimation parameters, in order to improve the dilution of precision and probability of position fix. The GGTO and GPS-to-GLONASS time offset are estimated in full GNSS visibility conditions, and these estimates are then re-used for partial and low visibility conditions. The GNSS pseudoranges are weighted according to the C/N_0 and satellite elevation, as in [16].

- **Hybrid navigation configuration**: The EKF is initialised with an approximate vehicle location obtained from the RINEX file. The matrix $\mathbf{P}$ is initialised to a large value, and the covariance matrix $\mathbf{Q}$ is defined by $\sigma_{\mathrm{pv}} = 10$ meters, $\sigma_{\mathrm{t}} = 10$ meters and $\sigma_{\mathrm{dt}} = 0.1$ meters. The weighting values of the covariance matrix $\mathbf{R}$ are defined with the square error between the observed ranges $\boldsymbol{\rho}$ (obtained from the previous location and the current satellite positions) and the estimated ranges $\hat{\boldsymbol{\rho}}$ (from the EKF algorithm), i.e., $\mathbf{R} = \mathrm{diag}\left((\boldsymbol{\rho} - \hat{\boldsymbol{\rho}})^2\right)$. This configuration does not include any weighting factor between GNSS and LTE pseudoranges.

4.2 Cell Site Location Accuracy

The location of the cell sites is estimated by considering an opportunistic receiver integrated in a vehicle, which follows the urban trajectory shown in Figure 3(a). The results obtained with the LS algorithm are shown in Table 3, only for those BS position solutions that converge with a RMSE below 100 meters. These results are evaluated considering the total angle of the receiver trajectory around the BS, which is called swath angle. As it is shown in Table 3, the cell site mapping significantly improves its performance for a minimum swath angle of 90 degrees, resulting in a cell site location accuracy around 8 meters. Despite the random trajectory of the vehicle, most of the BSs are covered with a swath angle greater than 90 degrees. Similar BS location accuracies are provided in public databases, such as around 15 meters from the Dutch Antenna bureau [23], which are obtained with GNSS receivers. Thus, a representative value of the BS location accuracy can be defined to 10 meters for opportunistic approaches.

Table 3 Average RMSE of the location accuracy of LTE BSs in the urban street scenario, for those LS solutions with a RMSE below 100 meters, i.e., 120 out of 137 BSs.

Swath angle ($^\circ$)	Number of BSs	RMSE (m)
< 45	23	43.63
> 45 (up to 90)	30	32.28
> 90	67	8.14

4.3 Multi-GNSS Positioning Performance

The position computation with the WLS requires a minimum of three observables plus one extra observable per constellation, resulting in six estimation parameters when using GPS, Galileo and GLONASS. Thus, the stand-alone WLS algorithm has severe performance degradation for partial and low visibility conditions. As it is shown in Table 4, the stand-alone WLS achieves a probability of position fix equal to 93.53%, due to the high percentage of partial and low visibility occasions. In order to improve the positioning performance, the WLS is assisted with the GGTO and GPS-to-GLONASS clock offset estimated during full visibility conditions. The re-use of these estimated offsets, i.e., assisted WLS algorithm, improves the dilution of precision of the position problem, resulting in an improvement of 4.18% in the probability of fix while maintaining a similar position accuracy. These results are also compared with the stand-alone EKF algorithm, which estimates and predicts the full set of parameters. As it can be seen, the prediction step of this navigation filter achieves a position availability of 100%, at the expense of decreasing the position accuracy in the 50% and 67% percentiles, due to epochs with very few and poor observables. Future work is aimed at implementing the assisted approach with the EKF, in order to improve the achievable accuracy, by reducing the number of estimation parameters for partial and low visibility conditions.

Table 4 Positioning performance with and without re-using the GGTO and GPS-to-GLONASS time offset in the urban street scenario.

Algorithm	Prob. fix (%)	CDF 2D position error (m) 50%	67%	95%
Stand-alone WLS	93.53	2.55	3.62	43.06
Assisted WLS	97.71	2.65	3.86	42.11
Stand-alone EKF	100	3.03	4.65	23.47

4.4 Impact of LTE Network Density and Inaccuracies

This section assesses the impact of the network density and inaccuracies in the LTE positioning performance of the vehicle with the EKF algorithm. The density of LTE BSs is first evaluated by considering four and eight BSs for the urban street

Table 5 Impact of LTE network density on the EKF navigation performance with 10 MHz LTE signals.

LTE configuration	Prob. fix (%)	CDF 2D position error (m) 50%	67%	95%
Urban street, 4 BS	100.00	9.66	12.73	30.09
Road, 4 BS	100.00	10.58	13.90	28.62
Urban street, 8 BS	100.00	6.35	8.29	15.11
Road, 8 BS	100.00	7.82	9.75	18.42

and road scenarios. As it can be seen in Table 5, the LTE positioning accuracy is better for the urban street scenario than for the road scenario. This is because the higher density of BSs in the urban scenarios increases the probability of selecting those BSs with a better HDOP. In addition, the use of eight LTE measurements results in a position accuracy around 15 meters for 95% of the epochs, which is equivalent to the nominal LTE position error due to standard multipath channels. Thus, the deployment of dedicated LTE BSs along the road, such as road-side units (RSU), is expected to achieve (at least) the nominal cellular localization accuracy in urban and road scenarios. In this sense, the use of eight LTE BSs is assumed for the rest of the positioning evaluation.

Since the BS position may be obtained from a public database, the BS may not be perfectly located. In this work, the reference BS position are assumed to be precisely known for the assisted approach. In the opportunistic approach, the BS position error is simulated by displacing the reference BS position in a certain direction every epoch. This direction is defined by a random uniformly distributed angle between 0 and 359 degrees. The resulting probability density function (PDF) of this BS angle error is shown in Figure 4(a). Considering representative BS position errors (i.e., of 10 meters), the impact of the BS position error is relatively low on the LTE positioning performance, as it is summarized in Table 6. For instance, a BS position error of 10 meters increases only the vehicle position error in 2 meters at 95% of the cases of the urban scenario.

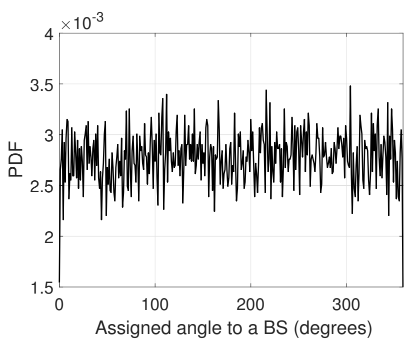

(a) PDF of BS angle error

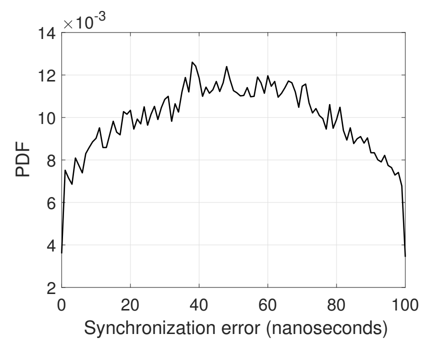

(b) Synchronization offset of 50 ns

Fig. 4 Distribution of network inaccuracies for the assessment of the opportunistic navigation approach.

In addition, the LTE networks are not perfectly synchronized. Similarly to [5], we model the network synchronization error with a truncated Gaussian distribution. This distribution has a mean and standard deviation equal to T_1 over a range of values equal to $T_2 = 2 \cdot T_1$. As an example, the PDF of the network synchronization errors for $T_1 = 50$ ns is shown in Figure 4(b). Let us consider that the opportunistic LTE navigation solution has residual synchronization errors with $T_1 = [10, 50, 100]$ ns, and these synchronization errors are added every epoch to the simulated ToA measurements. As it is shown in Table 6, network synchronization errors above 50 ns have a significant impact on the LTE positioning performance, because these errors are larger than the multipath ranging errors (i.e., in the order of 15 meters for this simulation). Therefore, network inaccuracies are expected to limit the achievable positioning performance of opportunistic approaches.

4.5 Hybrid Navigation Performance

This section evaluates the positioning performance of GNSS, LTE V2I and hybrid solutions with assisted and opportunistic approaches. The assisted approach assumes perfect network synchronization and precise knowledge of the BS locations. The opportunistic approach is characterized by a certain residual synchronization error equal to 50 ns and BS location errors equal to 10 meters, according to the representative values discussed in the previous section. In addition, a high density of BSs is considered, thus eight LTE BSs are used in the navigation algorithm. In both approaches, the PVT is computed by estimating the receiver clock offset with respect to each GNSS constellation and the LTE network.

Table 6 Impact of network inaccuracies on the LTE navigation performance in the urban street scenario.

BS location error (m)	Network sync. error (ns)	CDF 2D position error (m) 50%	67%	95%
0	0	6.35	8.29	15.11
5	0	6.61	8.64	15.59
10	0	7.19	9.39	17.10
20	0	9.99	13.00	22.83
0	10	6.44	8.35	15.25
0	50	7.67	9.96	17.87
0	100	10.78	13.81	24.03

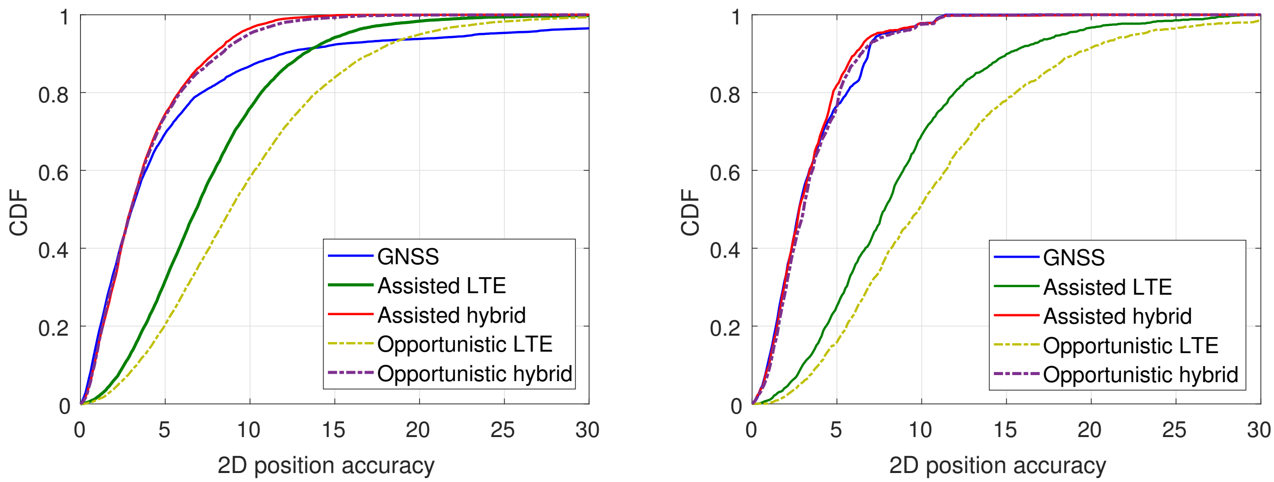

(a) Urban street scenario.

(b) Road scenario.

Fig. 5 EKF positioning performance with GNSS, LTE and hybrid solutions for assisted and opportunistic approaches.

The positioning results are summarized for the urban street and road scenarios in Table 7 and in Figure 5. First, the assisted LTE approach has a clear improvement with respect to the opportunistic LTE approach, whose accuracy is degraded due the combination of the two network inaccuracies considered. Second, the LTE positioning accuracy is worse in the road scenario than in the urban scenario, due to sparsity or low density of BSs. Third, the multi-GNSS solution achieves a nominal position accuracy of 7.6 meters in road scenarios, while it has a poor performance in urban environments. The use of broadcast ephemeris limits the achievable accuracy of this approach in open-sky conditions, while the high number of estimation parameters reduces the positioning capabilities in low visibility conditions. Thus, future work is aimed at exploiting precise GNSS corrections and at reducing the number of estimation parameters, e.g. by re-using the constellation clock offsets, the vehicle height or the velocity. Finally, the hybrid solutions provide the best results, having similar performance between assisted and opportunistic approaches. This is because the achievable hybrid position accuracy is mainly dominated (in these cases) by the GNSS position accuracy. In addition, full position availability is obtained for every approach thanks to the EKF navigation, which is able to estimate and predict the PVT even in epochs with very few pseudoranges. This full probability fix is achieved at the expense of reducing the achievable position accuracy, since the position error is expected to increase for those epochs with low satellite visibility and few LTE BSs. As a result, the achievable hybrid position accuracy is around 7 and 9 meters at the 95% of the cases for road and urban scenarios, respectively, which is mainly dominated by the multi-GNSS positioning accuracy. However, this accuracy is still high for autonomous vehicle applications. Thus, future work should consider further enhancements based on the adoption of 5G enabling technologies (e.g. high signal bandwidth, high carrier frequencies, or large number of antennas) with dedicated V2X networks, precise-point positioning (PPP) or real-time kinematic (RTK) approaches with GNSS, further optimization of the EKF navigation solution, and the hybrid fusion of multiple sensor technologies.

Table 7 EKF navigation performance for urban street and road scenarios.

Configuration	Scenario	Prob. fix (%)	CDF 2D position error (m) 50%	67%	95%
GNSS	Urban	100.00	3.03	4.65	23.47
	Road	100.00	2.76	3.95	7.58
Assisted LTE	Urban	100.00	6.35	8.29	15.11
	Road	100.00	7.82	9.75	18.42
Assisted hybrid	Urban	100.00	2.96	4.21	9.29
	Road	100.00	2.78	3.89	7.26
Opportunistic LTE	Urban	100.00	8.90	11.35	19.97
	Road	100.00	9.84	12.55	22.74
Opportunistic hybrid	Urban	100.00	3.00	4.30	9.86
	Road	100.00	3.04	4.05	8.15

5 CONCLUSION

This paper has studied the performance limits of conventional hybrid GNSS and LTE V2I positioning solutions for autonomous vehicle applications. A software tool is presented to post-process and evaluate the combination of field GNSS pseudoranges and simulated LTE measurements, by considering the location of deployed base stations (BSs). Representative network inaccuracies, i.e., network synchronization errors of 50 ns and BS location errors of 10 meters, are shown to have a clear impact on the opportunistic LTE positioning performance. Thus, the correction of these network inaccuracies (i.e., assisted approach) is necessary to achieve the best LTE positioning performance. As a result, the assisted hybrid navigation achieves the best performance among these conventional approaches, with a position accuracy around 7 and 9 meters at the 95% percentile in urban and road scenarios, respectively. However, this accuracy is not enough to fulfil the stringent location requirements for autonomous vehicle localization. Future work should introduce further enhancements in 4G and 5G networks with the provision of precise corrections for GNSS and LTE, the exploitation of emerging 5G technologies, and the hybrid fusion with additional sensors.

ACKNOWLEDGMENT

The content of the present article reflects solely the authors view and by no means represents the official European Space Agency (ESA) view. This work was supported by the ESA under NPI programme No. 4000110780/14/NL/AK, and by the Spanish Ministry of Science and Innovation project TEC2014-53656-R.

REFERENCES

[1] 5G-PPP, “5G automotive vision,” White Paper, Oct. 2015.

[2] 3GPP TS 36.211, *Physical channels and modulation*, Std., Rel. 9, 2010.

[3] H. Wymeersch, G. Seco-Granados, G. Destino, D. Dardari, and F. Tufvesson, “5G mm-Wave positioning for vehicular networks,” *IEEE Wireless Communications Magazine*, to appear, 2017.

[4] FCC, “Fourth report and order on wireless E911 location accuracy requirements,” Tech. Rep., Jan. 2015.

[5] 3GPP TR 37.857, *Study on indoor positioning enhancements for UTRA and LTE*, Std., Rel. 13, Dec. 2015.

[6] ECC Report 225, “Establishing criteria for the accuracy and reliability of the caller location information in support of emergency services,” CEPT Electronic Communications Committee, Tech. Rep., Oct. 2014.

[7] J. A. del Peral-Rosado, J. A. López-Salcedo, G. Seco-Granados, P. Crosta, F. Zanier, and M. Crisci, “Downlink synchronization of LTE base stations for opportunistic ToA positioning,” in *Proc. ICL-GNSS*, June 2015.

[8] M. Driusso, C. Marshall, M. Sabathy, F. Knutti, H. Mathis, and F. Babich, “Vehicular position tracking using LTE signals,” *IEEE Transactions on Vehicular Technology*, vol. 66, no. 4, pp. 3376–3391, 2017.

[9] K. Shamaei, J. Khalife, and Z. Kassas, “Performance characterization of positioning in LTE systems,” in *Proc. ION GNSS*, 2016.

[10] Z. M. Kassas, J. Khalife, K. Shamaei, and J. Morales, “I hear, therefore I know where I am: Compensating for GNSS limitations with cellular signals,” *IEEE Signal Processing Magazine*, vol. 34, no. 5, pp. 111–124, Sep. 2017.

[11] C. Botteron, E. Firouzi, and P.-A. Farine, “Performance analysis of mobile station location using hybrid GNSS and cellular network measurements,” in *Proc. ION GNSS*, 2004.

[12] G. De Angelis, G. Baruffa, and S. Cacopardi, "GNSS/cellular hybrid positioning system for mobile users in urban scenarios," *IEEE Trans. Intell. Transp. Syst.*, vol. 14, no. 1, pp. 313–321, Mar. 2013.

[13] C. Mensing, S. Sand, and A. Dammann, "Hybrid data fusion and tracking for positioning with GNSS and 3GPP-LTE," *International Journal of Navigation and Observation*, vol. 2010, 2010.

[14] J. A. del Peral-Rosado, R. Estatuet-Castillo, J. Míguez-Sánchez, M. Navarro-Gallardo, J. A. García-Molina, J. A. López-Salcedo, G. Seco-Granados, F. Zanier, and M. Crisci, "Performance analysis of hybrid GNSS and LTE Localization in urban scenarios," in *Proc. NAVITEC*, Dec. 2016.

[15] RP-162521, "New SID: Study on LTE vehicular positioning technologies," Intel Corporation, RAN-74, Dec. 2016.

[16] A. M. Herrera, H. F. Suhandri, E. Realini, M. Reguzzoni, and M. C. de Lacy, "goGPS: open-source MATLAB software," *GPS Solutions*, vol. 20, no. 3, pp. 595–603, 2016.

[17] J. A. del Peral-Rosado, J. M. Parro-Jiménez, J. A. López-Salcedo, G. Seco-Granados, P. Crosta, F. Zanier, and M. Crisci, "Comparative results analysis on positioning with real LTE signals and low-cost hardware platforms," in *Proc. NAVITEC*, Dec. 2014.

[18] A. Leick, *GPS Satellite Surveying*, 2nd ed. John Wiley & Sons, Inc., New York, 2004.

[19] J. Saastamoinen, "Contributions to the theory of atmospheric refraction," *Bulletin Géodésique (1946-1975)*, vol. 107, no. 1, pp. 13–34, 1973.

[20] B. W. Remondi, "Computing satellite velocity using the broadcast ephemeris," *GPS solutions*, vol. 8, no. 3, pp. 181–183, 2004.

[21] J. Míguez-Sánchez, J. V. Perello-Gisbert, R. Orus-Pérez, J. A. García-Molina, P. Zoccarato, L. Ries, X. Serena, F. González, G. Seco-Granados, and M. Crisci, "Real-time multi-GNSS PPP kinematic performance assessment in challenging scenarios," in *Proc. NAVITEC*, Dec. 2016.

[22] 3GPP TR 36.942, *RF system scenarios*, Std., Rel. 13, Jan. 2016.

[23] Antenna Bureau, Radiocommunications Agency of The Netherlands, http://www.antenneregister.nl/register, [Online; accessed 31-Dec-2015].

[24] 3GPP TS 36.101, *UE radio transmission and reception*, Std., Rel. 13, Jan. 2016.